Arabian Journal of Chemistry (2019) **12**, 4365–4376

King Saud University

Arabian Journal of Chemistry

www.ksu.edu.sa
www.sciencedirect.com

ORIGINAL ARTICLE

Iminecalix[4]arenes: Microwave-assisted synthesis, X-ray crystal structures, and anticandidal activity

Cleiton M. da Silva [a], Danielle L. da Silva [b], Thais F.F. Magalhães [b], Rosemeire B. Alves [a], Maria A. de Resende-Stoianoff [b], Felipe T. Martins [c], Ângelo de Fátima [a,*]

[a] *Grupo de Estudos em Química Orgânica e Biológica (GEQOB), Departamento de Química, Instituto de Ciências Exatas, Universidade Federal de Minas Gerais, Av. Pres. Antônio Carlos, 6627, Belo Horizonte, MG 31270-901, Brazil*
[b] *Departamento de Microbiologia, Instituto de Ciências Biológicas, Universidade Federal de Minas Gerais, Av. Pres. Antônio Carlos, 6627, Belo Horizonte, MG 31270-901, Brazil*
[c] *Instituto de Química, Universidade Federal de Goiás, Campus Samambaia, CP 131, Goiânia, GO 74001-970, Brazil*

Received 28 January 2016; accepted 20 June 2016
Available online 27 June 2016

KEYWORDS

Calix[4]arene;
Aldimine;
Iminecalix[4]arenes microwave-assisted synthesis;
Antifungal activity;
X-ray crystal structure;
Pinched cone conformation

Abstract In this study, six iminecalix[4]arenes were synthesized and the crystal structures of two of the iminecalix[4]arenes were also determined. Iminecalix[4]arene adopts a strongly pinched cone conformation with two upper rim substituents pointing toward and the other two pointing away from the aromatic cavity. This uncommon conformation is stabilized by an intramolecular π...π interaction between the phenyl rings from the upper rim substituents pointing inwards the cone. In addition, phenyl rings from the substituent groups are not coplanar with respect to the calixarene phenyl rings holding them. The compounds, as well as their respective monomeric units, were evaluated for their antifungal activities against *Candida* strains. All the synthesized iminecalix[4]arenes were found to cause higher inhibition of all tested *Candida* strains than their respective monomers. The ratio between the minimal inhibitory concentration (MIC) of a monomer and the corresponding iminecalix[4]arene ranged from 2.05 to 36.50. Furthermore, the iminecalix[4]arene bearing nitrofuran group exhibited low MIC values comparable to that of fluconazole. Thus, this compound was twice more active than fluconazole against *Candida krusei*.

1. Introduction

In the last few decades, calixarenes and their functionalized derivatives have attracted increasing attention due to their technological and biological applications (Consoli et al., 2006, 2011; Motornaya et al., 2006; Mourer et al., 2010, 2012; Patel et al., 2012; Ukhatskaya et al., 2013; Pelizzaro-Rocha et al., 2013), particularly as platforms for the development of new drugs (de Fátima et al., 2009; Varejão et al., 2013; Lappchen et al., 2015; Tauran et al., 2015; Giuliani et al., 2015). The

* Corresponding author. Fax: +55 31 3409 5700.
E-mail address: adefatima@qui.ufmg.br (Â. de Fátima).
Peer review under responsibility of King Saud University.

Production and hosting by Elsevier

http://dx.doi.org/10.1016/j.arabjc.2016.06.013
1878-5352

highly organized structures of the calixarenes could give rise to interesting synergistic effects that are not observed in their respective monomeric units. In this sense, studies conducted in 2007 by Grare and coworkers indicate that a *p*-guanidinoethylcalix[4]arene shows broad spectrum antibacterial activity, while no antibacterial activity was observed with the corresponding monomer guanidinoethylphenol (Grare et al., 2007). Two years later, the same group reported that other three *p*-guanidinoethylcalix[4]arenes also possess, in general, better antibacterial activities than their corresponding monomers (Mourer et al., 2009). Characteristics such as easy-to-perform in multi-gram scale synthesis from low cost precursors, chemical and thermal stability, and easiness of functionalization make calixarenes versatile platforms for the development of a wide range of compounds with applications in medicinal chemistry (Křenek et al., 2007; Deshayes and Gref, 2014; Guo and Liu, 2014; Kamboh et al., 2014; Du et al., 2015).

Fungi have remained neglected pathogens in terms of drug discovery (Sundriyal et al., 2006; Choi et al., 2014) despite their highlighted clinical relevance (Andriole et al., 1999; Ascioglu et al., 2002; Nucci et al., 2005; Franco-Paredes et al., 2015). The *Candida* species are certainly the most important opportunistic fungal pathogens for humans (Pfaller et al., 2006; Pfaller and Diekema, 2007; Whibley and Gaffen, 2015). Candidiasis may range from non-life threatening mucocutaneous illnesses to invasive processes (Pappas et al., 2004; Sparber and LeibundGut-Landmann, 2015). Both mucosal and deep tissue infections are mainly caused by *C. albicans* (Pappas et al., 2004). *Candida* species other than *albicans* have been assumed to be the pathogens of nosocomial infections in immunocompromised patients (Walsh et al., 1995; Girmenia et al., 1996; Whibley and Gaffen, 2015). Concerning the currently available antifungal drugs, most active compounds exhibit drawbacks, such as fungi resistance, toxicity, limited efficacy, and high cost (Sundriyal et al., 2006; Rizi et al., 2015). This scenario clearly indicates that research on new antifungal agents is required.

Aldimines are known to exhibit remarkable biological properties (Abdallah et al., 2010; da Silva et al., 2011a; Sztanke et al., 2013; Matar et al., 2015; Amnerkar et al., 2015; Hisaindee et al., 2015). Recently, our research group demonstrated that aldimines show interesting inhibitory activity against a variety of pathogenic fungi, including *Candida*, *Aspergillus*, and *Cryptococcus* species (da Silva et al., 2011b; Magalhães et al., 2013; Gasparto et al., 2015). Calixarenes have also demonstrated antifungal profiles (Paquet et al., 2006; Patel et al., 2012; de Oliveira et al., 2012). In this context, the synthesis of hybrid calixarene–aldimines presents a promising strategy for obtaining new compounds with enhanced antifungal activity. Calixarene-based aldimines have been successfully synthesized previously as precursors of anion receptor in water (Klimentová and Vojtíšek, 2007). We here report the microwave-assisted synthesis of six iminecalix[4]arenes (compounds **6**–**11**; Scheme 1) and their respective monomeric units (compounds **14**–**19**; Scheme 2). Crystal structures of two of the synthesized compounds were determined. The antifungal activities against six species of *Candida* are also described.

2. Experimental

2.1. Chemistry

2.1.1. General procedures

All chemicals were obtained from commercially available sources and used without further purification. Melting points (uncorrected) were determined on Mettler FP 80 HT apparatus. Infrared spectra were recorded on a Perkin Elmer Spectrum One spectrophotometer (ATR). ^{1}H and ^{13}C NMR spectra were recorded on a Bruker AVANCE DPX-200 spectrometer or a VARIAN MERCURY-300 spectrometer in $CDCl_3$. High-resolution mass spectra were recorded on a Shimadzu LCMS-IT-TOF instrument. Compounds **5** and **13** (Schemes 1 and 2) were synthesized according to procedures reported in the literature (Li et al., 2009, 2011).

Well-shaped single crystals of compounds **7** and **10** (Schemes 1 and 2) with dimensions of $0.32 \times 0.21 \times 0.05\ mm^3$ and $0.25 \times 0.012 \times 0.05\ mm^3$ were exposed to the X-ray beam (Mo Kα or Cu Kα radiation from IμS microsources with multilayer optics) at room temperature using a Bruker-AXS Kappa Duo diffractometer equipped with an APEX II CCD detector. The diffraction frames were recorded by φ and ω scans using APEX2 (Bruker, 2012), and this software package was also employed for treatment of the raw dataset. The structures were solved using direct methods of phase retrieval with SHELXS-97 (Sheldrick, 2008). Identification of C, O, and N atoms was done directly from the Fourier synthesis maps, which were then refined with

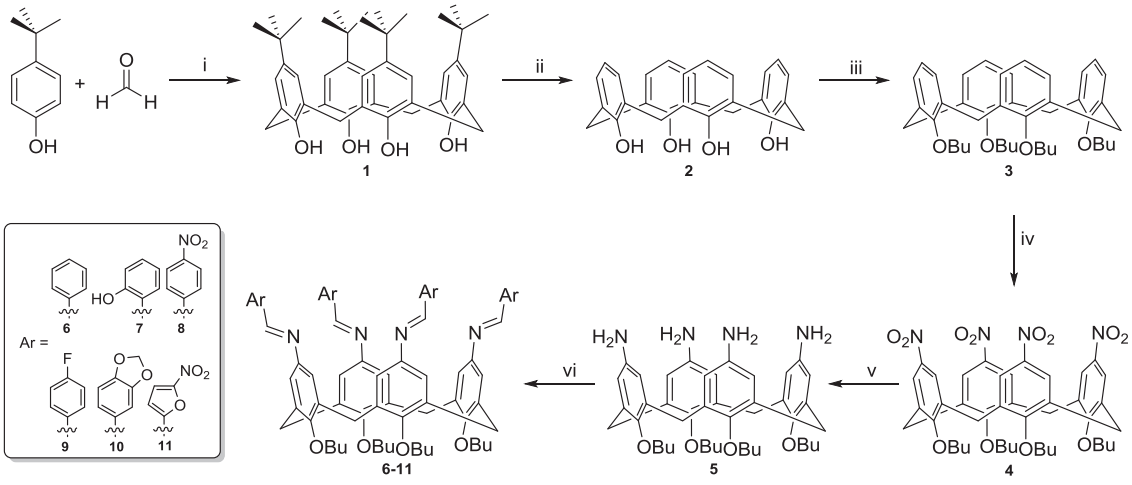

Scheme 1 Synthesis of iminecalix[4]arenes **6**–**11**. (i) Diphenyl ether, NaOH, 260 °C, 56%; (ii) $AlCl_3$, phenol, toluene, r.t., 80%; (iii) NaH, *n*-BuBr, DMF, 80 °C, 60%; (iv) $HOAc/HNO_3$, r.t., 54%; (v) $N_2H_4{\cdot}H_2O$, Pd/C, EtOH, 80 °C, 99%; (vi) ArCHO, EtOH, microwave irradiation, 52–90%.

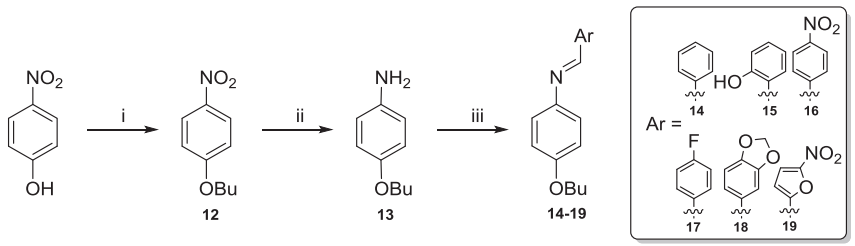

Scheme 2 Synthesis of the monomer units **14**–**19**. (i) K_2CO_3, *n*-BuBr, MeCN, 80 °C, 94%; (ii) $N_2H_4{\cdot}H_2O$, Pd/C, EtOH, 80 °C, 99%; (iii) ArCHO, EtOH, microwave irradiation, 69–88%.

anisotropic atomic displacement parameters (ADPs). All refinements were performed using the full-matrix least squares method on F^2 using SHELXL-97 (Sheldrick, 2008). Hydrogen atoms were stereochemically positioned with fixed individual isotropic ADPs based on the equivalent isotropic ADP of the parent non-hydrogen atom [Uiso(H) = 1.2 Ueq or 1.5 Ueq (only in the case of methyl carbons and hydroxyl oxygens)] using a riding model with fixed C—H bond lengths of either 0.93 Å (Csp^2), 0.97 Å (Csp^3 in methylene groups), or 0.96 Å (Csp^3 in methyl groups) and a O—H bond length of 0.82 Å. The MERCURY (Macrae et al., 2008) and ORTEP-3 (Farrugia, 2012) programs accessed through the WinGX (Farrugia, 2012) software package were used to prepare structure illustrations. CCDC reference numbers 1439308 and 1439309 contain the crystal data for compounds **7** and **10**, respectively.

Additionally, a positional disorder in the upper rim substituent at calixarene phenyl rings 2 and 4 was found in the case of compound **7** and was refined using the classical split-atom approach. Two sets of atomic sites were found for each substituent. Their major occupancies were constrained to 55% and 60% for the substituents at phenyl rings 2 and 4, respectively. The minor occupancy factors were constrained to 45% and 40%, and their labels followed those from major ones but ended with apostrophe.

Crystal data for compound 7. $C_{72}H_{76}N_4O_8$, MW = 1125.37, monoclinic, a = 12.405(5) Å, b = 30.137(12) Å, c = 17.782 (7) Å, β = 101.502(9)°, V = 6514(4) Å^3, T = 297(2) K, space group $P2_1/c$, Z = 4, Dc = 1.148 g cm^{-3}, μ (Mo Kα) = 0.075 mm^{-1}, θ-range for data collection = 1.35–25.49, $-14 \leqslant h \leqslant 15$, $-36 \leqslant k \leqslant 33$, $-9 \leqslant l \leqslant 21$, 53,392 reflections collected, 11,865 unique (R_{int} = 0.0706), 4797 with $I > 2\sigma(I)$, completeness to θ_{max} = 97.9%, F_{000} = 2400, 918 parameters refined, S = 1.145, $R_1(I > 2\sigma(I))$ = 0.1262, wR_2(all data) = 0.3987, largest diff. peak/hole = 0.714/−0.463 e Å^{-3}.

*Crystal data for compound **10***. $C_{76}H_{76}N_4O_{12}$, MW = 1237.41, monoclinic, a = 13.713(4) Å, b = 28.956(9) Å, c = 17.592(6) Å, β = 103.184(18)°, V = 6801(4) Å^3, T = 297(2) K, space group $P2_1/c$, Z = 4, Dc = 1.209 g cm^{-3}, μ (Mo Kα) = 0.082 mm^{-1}, θ-range for data collection = 1.68–25.45, $-16 \leqslant h \leqslant 16$, $-34 \leqslant k \leqslant 34$, $-21 \leqslant l \leqslant 19$, 70,533 reflections collected, 12,361 unique (R_{int} = 0.0685), 6191 with $I > 2\sigma(I)$, completeness to θ_{max} = 98.2%, F_{000} = 2624, 833 parameters refined, S = 1.084, $R_1(I > 2\sigma(I))$ = 0.0861, wR_2(all data) = 0.2574, largest diff. peak/hole = 0.360/−0.321 e Å^{-3}.

*Unit cell data for compound **11***. monoclinic, a = 14.79(3) Å, b = 33.55(9) Å, c = 13.41(3) Å, β = 100.68(8)°, V = 6539 (27) Å^3, T = 297(2) K, θ-range for data collection (Cu Kα) = 7.22–42.04, $-10 \leqslant h \leqslant 9$, $-24 \leqslant k \leqslant 27$, $-7 \leqslant l \leqslant 11$, 3083 reflections collected, 2684 unique (R_{int} = 0.0479), 1241 with $I > 2\sigma(I)$.

*2.1.2. General procedure for synthesis of iminecalix[4]arenes **6**–**11***

Compound **5** (0.15 mmol) and respective aldehydes (0.66 mmol, 1.1 equivalents for amino group) were solubilized in ethanol (20 mL). The mixtures were irradiated in a Discover CEM® reactor for 20 min at reflux temperature. After the reaction was complete, the products were isolated by filtration.

Iminecalix[4]arene 6

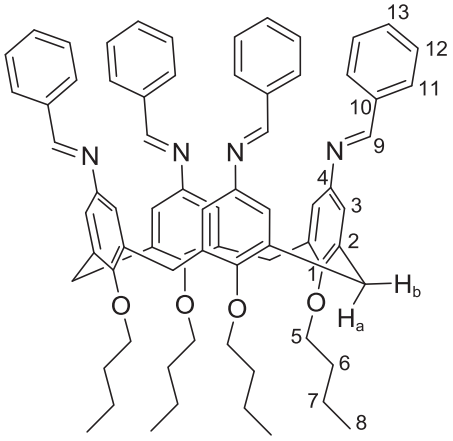

Yield: 52%. Yellow solid. Mp: 136.3–137.8 °C. IR (ATR, cm^{-1}) $\bar{\nu}$: 2957, 2929, 2869, 1624, 1576, 1457, 1378, 1310, 1237, 1205, 1117, 1069, 1023, 999, 967, 884, 849, 753. ^{1}H NMR (300 MHz, $CDCl_3$): δ 1.03 (t, 12H, $J_{8,7}$ = 7.4 Hz, H_8), 1.49 (sex, 8H, $J_{7,6} = J_{7,8}$ = 7.4 Hz, H_7), 1.97 (quin, 8H, $J_{6,5} = J_{6,7}$ = 7.4 Hz, H_6), 3.25 (d, 4H, $J_{b,a}$ = 13.0 Hz, H_b), 3.96 (t, 8H, $J_{5,6}$ = 7.4 Hz, H_5), 4.52 (d, 4H, $J_{a,b}$ = 13.0 Hz, H_a), 6.79 (s, 8H, H_3), 7.20–7.33 (m, 12H, H_{12}, H_{13}), 7.66 (dd, 8H, $J_{11,12}$ = 8.4 Hz, $J_{11,13}$ = 1.5 Hz, H_{11}), 8.14 (s, 4H, H_9). ^{13}C NMR (75 MHz, $CDCl_3$): δ 14.4 (C_8), 19.6 (C_7), 31.5, 32.5 (C_6, CH_2), 75.4 (C_5), 121.1 (C_3), 128.6, 128.8 (C_{11}, C_{12}), 130.8 (C_{13}), 135.5 (C_2), 136.5 (C_{10}), 146.5 (C_4), 155.4 (C_1), 158.9 (C_9). HRMS (ESI, IT-TOF) calculated for $C_{72}H_{77}N_4O_4^+$: 1061.5939; found: 1061.6016.

Iminecalix[4]arene 7

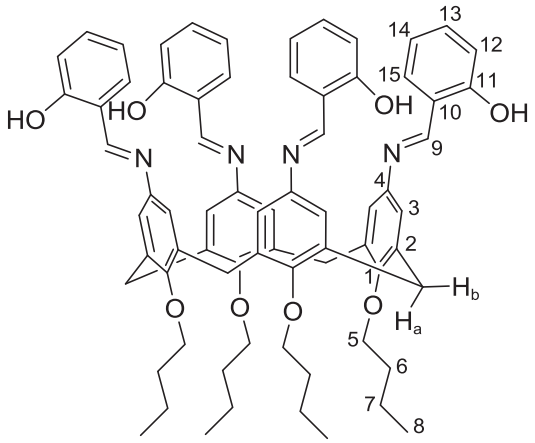

Yield: 85%. Yellow solid. Mp: 285.5–286.8 °C. IR (ATR, cm^{-1}) $\bar{\nu}$: 2957, 2869, 1614, 1573, 1462, 1276, 1207, 1150, 1117, 1065, 1003, 958, 868, 794. ^{1}H NMR (300 MHz, $CDCl_3$): δ 1.05 (t, 12H, $J_{8,7}$ = 7.4 Hz, H_8), 1.50 (sex, 8H, $J_{7,6} = J_{7,8}$ = 7.4 Hz, H_7), 1.96 (quin, 8H, $J_{6,5} = J_{6,7}$ = 7.4 Hz, H_6), 3.28 (d, 4H, $J_{b,a}$ = 13.3 Hz, H_b), 3.98 (t, 8H, $J_{5,6}$ = 7.4 Hz, H_5), 4.54 (d, 4H, $J_{a,b}$ = 13.3 Hz, H_a), 6.71–6.79 (m, 16H, H_3, H_{12}, H_{14}), 7.14–7.24 (m, 8H, H_{13}, H_{15}), 8.28 (s, 4H, H_9), 13.25 (s, 4H, OH). ^{13}C NMR (75 MHz, $CDCl_3$): δ 14.3 (C_8), 19.6 (C_7), 31.6, 32.4 (C_6, CH_2), 75.5 (C_5), 117.0, 118.8 (C_{12}, C_{14}), 119.4 (C_{10}), 121.1 (C_3), 132.1, 132.6 (C_{13}, C_{15}), 135.9 (C_2), 142.9 (C_4), 156.1 (C_{11}), 161.0 (C_1, C_9). HRMS (ESI, IT-TOF) calculated for $C_{72}H_{77}N_4O_8^+$: 1125.5736; found: 1125.5809.

Iminecalix[4]arene 8

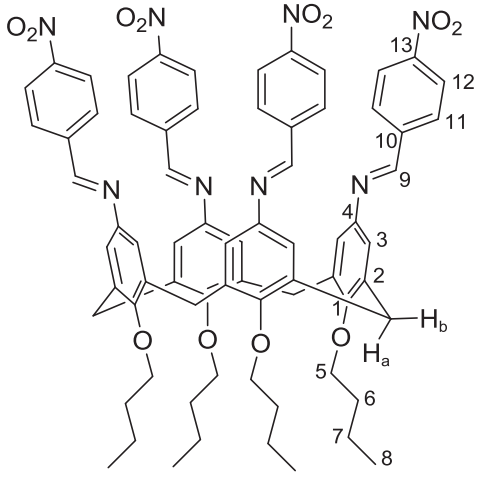

Yield: 90%. Yellow solid. Mp: 243.4–245.9 °C. IR (ATR, cm^{-1}) $\bar{\nu}$: 2930, 1597, 1519, 1456, 1291, 1207, 1106, 1065, 999, 975, 888, 850, 838, 747, 688. ^{1}H NMR (300 MHz, $CDCl_3$): δ 1.04 (t, 12H, $J_{8,7}$ = 7.4 Hz, H_8), 1.50 (sex, 8H, $J_{7,6} = J_{7,8}$ = 7.4 Hz, H_7), 1.96 (quin, 8H, $J_{6,5} = J_{6,7}$ = 7.4 Hz, H_6), 3.29 (d, 4H, $J_{b,a}$ = 13.4 Hz, H_b), 3.99 (t, 8H, $J_{5,6}$ = 7.4 Hz, H_5), 4.54 (d, 4H, $J_{a,b}$ = 13.4 Hz, H_a), 6.77 (s, 8H, H_3), 7.80 (d, 2H, $J_{11,12}$ = 8.6 Hz, H_{11}) 8.09 (d, 2H, $J_{12,11}$ = 8.6 Hz, H_{12}), 8.23 (s, 1H, H_9). ^{13}C NMR (75 MHz, $CDCl_3$): δ 14.3 (C_8), 19.6 (C_7), 31.5, 32.5 (CH_2, C_6), 75.5 (C_5), 121.5 (C_3), 123.9 (C_{12}), 129.1 (C_{11}), 135.9 (C_2), 141.8, 145.2 (C_4, C_{10}), 148.9 (C_{13}), 155.5 (C_9), 156.7 (C_1). HRMS (ESI, IT-TOF) calculated for $C_{72}H_{73}N_8O_{12}^+$: 1241.5342; found: 1241.5656.

Iminecalix[4]arene 9

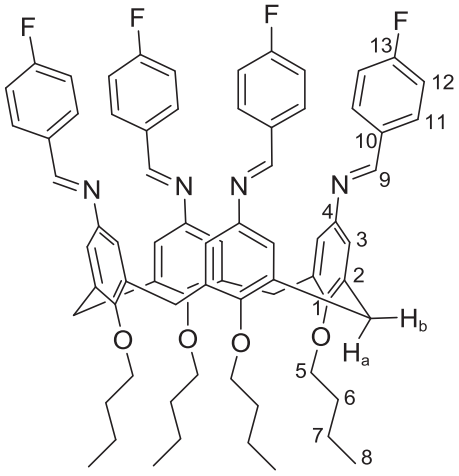

Yield: 73%. Yellow solid. Mp: 272.5–273.6 °C. IR (ATR, cm^{-1}) $\bar{\nu}$: 2956, 2870, 1625, 1601, 1587, 1507, 1457, 1378, 1293, 1151, 1067, 1025, 1000, 974, 956, 887, 858, 834. ^{1}H NMR (300 MHz, $CDCl_3$): δ 1.03 (t, 12H, $J_{8,7}$ = 7.4 Hz, H_8), 1.48 (sex, 8H, $J_{7,6} = J_{7,8}$ = 7.4 Hz, H_7), 1.96 (quin, 8H, $J_{6,5} = J_{6,7}$ = 7.4 Hz, H_6), 3.24 (d, 4H, $J_{b,a}$ = 13.2 Hz, H_b), 3.95 (t, 8H, $J_{5,6}$ = 7.4 Hz, H_5), 4.51 (d, 4H, $J_{a,b}$ = 13.2 Hz, H_a), 6.67 (s, 8H, H_3), 6.95 (t, 8H, $J_{12,11} = J_{12,F}$ = 8.6 Hz, H_{12}), 7.63 (dd, 8H, $J_{11,12}$ = 8.6 Hz, $J_{11,F}$ = 5.5 Hz, H_{11}), 8.06 (s, 4H, H_9). ^{13}C NMR (75 MHz, $CDCl_3$): δ 14.4 (C_8), 19.6 (C_7), 31.5, 32.5 (CH_2, C_6), 75.4 (C_5), 115.7 (d, $J_{12,F}$ = 21.9 Hz, C_{12}), 121.1 (C_3), 130.6 (d, $J_{11,F}$ = 8.6 Hz, C_{11}), 132.8 (d, $J_{10,F}$ = 2.9 Hz, C_{10}), 135.6 (C_2), 146.2 (C_4), 155.6 (C_1), 157.3 (C_9), 164.3 (d, $J_{13,F}$ = 251.6 Hz, C_{13}). HRMS (ESI, IT-TOF) calculated for $C_{72}H_{73}F_4N_4O_4^+$: 1133.5562; found: 1133.5650.

Iminecalix[4]arene 10

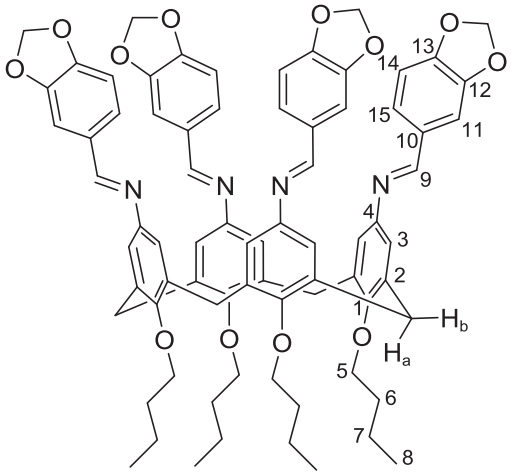

Yield: 78%. Brown solid. Mp: 195.0–196.2 °C. IR (ATR, cm^{-1}) $\bar{\nu}$: 2868, 1622, 1601, 1584, 1504, 1488, 1445, 1379, 1347, 1208, 1098, 1064, 1035, 1002, 933, 876, 801. ^{1}H NMR (300 MHz, $CDCl_3$): δ 1.02 (t, 12H, $J_{8,7}$ = 7.5 Hz, H_8), 1.48 (sex, 8H, $J_{7,6} = J_{7,8}$ = 7.5 Hz, H_7), 1.95 (quin, 8H, $J_{6,5} = J_{6,7}$ = 7.5 Hz, H_6), 3.22 (d, 4H, $J_{b,a}$ = 13.3 Hz, H_b), 3.93 (t, 8H, $J_{5,6}$ = 7.5 Hz, H_5), 4.48 (d, 4H, $J_{a,b}$ = 13.3 Hz, H_a), 5.97 (s, 8H, $OC\underline{H}_2O$), 6.64 (s, 8H, H_3), 6.69 (d, 4H, $J_{14,15}$ = 8.0 Hz, H_{14}), 7.04 (dd, 4H, $J_{15,14}$ = 8.0 Hz, $J_{15,11}$ = 1.3 Hz, H_{15}), 7.23 (d, 4H, $J_{11,15}$ = 1.3 Hz, H_{11}), 7.92 (s, 4H, H_9). ^{13}C NMR (75 MHz, $CDCl_3$): δ 14.3 (C_8), 19.6 (C_7), 31.5, 32.5 (C_6, CH_2), 75.3 (C_5), 101.6 ($O\underline{C}H_2O$), 106.9, 108.0 (C_{11}, C_{14}), 121.0 (C_3), 125.5 (C_{15}), 131.6 (C_{10}), 135.6 (C_2), 146.3, 148.1, 149.9 (C_4, C_{12}, C_{13}), 155.2 (C_1), 157.9 (C_9). HRMS (ESI, IT-TOF) calculated for $C_{76}H_{77}N_4O_{12}^+$: 1237.5533; found: 1237.5636.

Iminecalix[4]arene 11

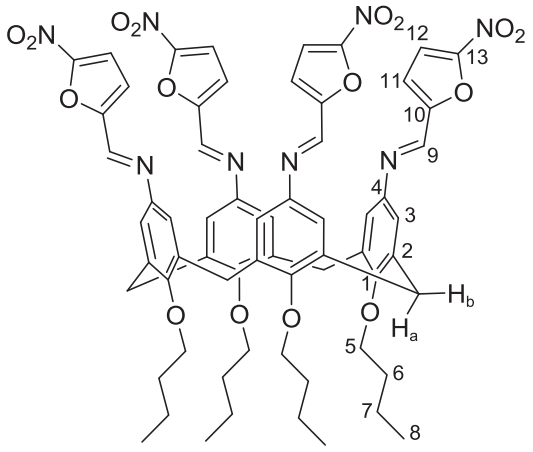

Yield: 69%. Brown solid. Mp: 181.2 °C (decomposition). IR (ATR, cm^{-1}) $\bar{\nu}$: 2957, 2931, 2870, 1571, 1523, 1487, 1458, 1394, 1282, 1294, 1211, 1117, 1064, 1017, 962, 880, 808, 736. ^{1}H NMR (300 MHz, $CDCl_3$): δ 1.03 (t, 12H, $J_{8,7}$ = 7.4 Hz, H_8), 1.48 (sex, 8H, $J_{7,6} = J_{7,8}$ = 7.4 Hz, H_7), 1.94 (quin, 8H, $J_{6,5} = J_{6,7}$ = 7.4 Hz, H_6), 3.25 (d, 4H, $J_{b,a}$ = 13.4 Hz, H_b), 3.97 (t, 8H, $J_{5,6}$ = 7.4 Hz, H_5), 4.50 (d, 4H, $J_{a,b}$ = 13.4 Hz, H_a), 6.74 (s, 8H, H_3), 7.01 (d, 4H, $J_{11,12}$ = 3.8 Hz, H_{11}), 7.28 (d, 4H, $J_{12,11}$ = 3.8 Hz, H_{12}), 8.10 (s, 4H, H_9). ^{13}C NMR (75 MHz, $CDCl_3$): δ 14.3 (C_8), 19.6 (C_7), 31.4, 32.5 (C_6, CH_2), 75.6 (C_5), 113.0, 113.9 (C_{11}, C_{12}), 121.8 (C_3), 135.9 (C_2), 144.2 (C_9), 144.3 (C_4), 152.4, 153.9 (C_{10}, C_{13}), 157.3 (C_1). HRMS (ESI, IT-TOF) calculated for $C_{64}H_{65}N_8O_{16}^+$: 1201.4513; found: 1201.4517.

*2.1.3. General procedure for synthesis of imines **14–19***

Compound **13** (0.15 mmol) and respective aldehydes (0.15 mmol) were solubilized in ethanol (20 mL). The mixtures were irradiated in a Discover Cem® reactor for 2 min at reflux temperature. After finished the reactions, the products were isolated by filtration.

(*E*)-*N*-(4-butoxyphenyl)-1-phenylmethanimine (14)

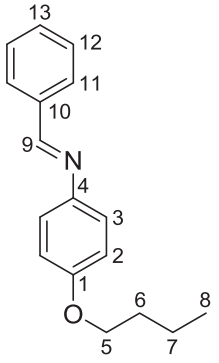

Yield: 72%. Light brown solid. Mp: 60.3–61.0 °C. IR (ATR, cm^{-1}) $\bar{\nu}$: 3061, 2954, 2933, 2870, 1623, 1575, 1503, 1473, 1449, 1396, 1369, 1244, 1189, 1112, 1036, 1007, 832, 752. ^{1}H NMR (200 MHz, $CDCl_3$): δ 0.97 (t, 3H, $J_{8,7}$ = 7.2 Hz, H_8), 1.49 (sex, 2H, $J_{7,6} = J_{7,8}$ = 7.2 Hz, H_7), 1.76 (quin, 2H, $J_{6,5} = J_{6,7}$ = 7.2 Hz, H_6), 3.95 (t, 2H, $J_{5,6}$ = 7.2 Hz, H_5), 6.90 (d, 2H, $J_{2,3}$ = 8.5 Hz, H_2), 7.22 (d, 2H, $J_{3,2}$ = 8.5 Hz, H_3), 7.38–7.49 (m, 3H, H_{12}, H_{13}), 7.87 (m, 2H, H_{11}), 8.45 (s, 1H, H_9). ^{13}C NMR (50 MHz, $CDCl_3$): δ 13.8 (C_8), 19.2 (C_7), 31.3 (C_6), 67.9 (C_5), 114.9 (C_2), 122.1 (C_3), 128.5, 128.6 (C_{11}, C_{12}), 130.9 (C_{13}), 136.4 (C_{10}), 144.6 (C_4), 157.8 (C_1), 158.1 (C_9). HRMS (ESI, IT-TOF) calculated for $C_{17}H_{20}NO^+$: 254.1539; found: 254.1438.

(*E*)-2-(((4-butoxyphenyl)imino)methyl)phenol (15)

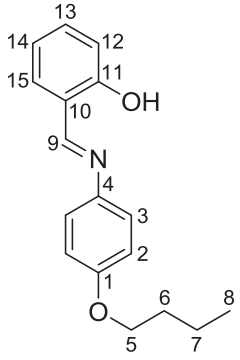

Yield: 80%. Yellow solid. Mp: 67.6–68.9 °C. IR (ATR, cm^{-1}) $\bar{\nu}$: 2956, 2932, 2872, 1615, 1570, 1491, 1470, 1456, 1394, 1280, 1242, 1186, 1150, 1110, 1068, 1025, 973, 909, 837. ^{1}H NMR (200 MHz, $CDCl_3$): δ 0.96 (t, 3H, $J_{8,7}$ = 7.2 Hz, H_8), 1.47 (sex, 2H, $J_{7,6} = J_{7,8}$ = 7.2 Hz, H_7), 1.75 (quin, 2H, $J_{6,5} = J_{6,7}$ = 7.2 Hz, H_6), 3.92 (t, 2H, $J_{5,6}$ = 7.2 Hz, H_5), 6.82–7.06 (m, 4H, H_2, H_{12}, H_{14}), 7.14–7.39 (m, 4H, H_3, H_{13}, H_{15}), 8.52 (s, 1H, H_9), 13.48 (s, 1H, OH). ^{13}C NMR (50 MHz, $CDCl_3$): δ 13.8 (C_8), 19.1 (C_7), 31.2 (C_6), 67.8 (C_5), 115.0 (C_2), 117.0, 118.8 (C_{12}, C_{14}), 119.3 (C_{10}), 122.1 (C_3), 131.8, 132.4 (C_{13}, C_{15}), 140.9 (C_4), 158.3 (C_1), 160.0, 160.8 (C_9, C_{11}). HRMS (ESI, IT-TOF) calculated for $C_{17}H_{20}NO_2^+$: 270.1489; found: 270.1396.

(*E*)-*N*-(4-butoxyphenyl)-1-(4-nitrophenyl)methanimine (16)

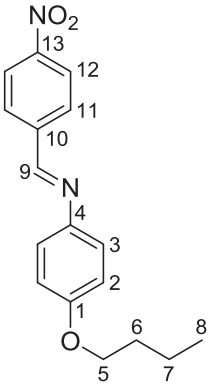

Yield: 88%. Yellow solid. Mp: 75.2–76.3 °C. IR (ATR, cm^{-1}) $\bar{\nu}$: 2958, 2927, 2873, 1624, 1597, 1582, 1520, 1504, 1284, 1244, 1164, 1106, 1064, 1023, 968, 804, 749, 718, 686. ^1H NMR (200 MHz, $CDCl_3$): δ 0.99 (t, 3H, $J_{8,7}$ = 7.2 Hz, H_8), 1.51 (sex, 2H, $J_{7,6} = J_{7,8}$ = 7.2 Hz, H_7), 1.79 (quin, 2H, $J_{6,5} = J_{6,7}$ = 7.2 Hz, H_6), 3.99 (t, 2H, $J_{5,6}$ = 7.2 Hz, H_5), 6.94 (d, 2H, $J_{2,3}$ = 8.0 Hz, H_2), 7.29 (d, 2H, $J_{3,2}$ = 8.0 Hz, H_3), 8.03 (d, 2H, $J_{11,12}$ = 8.2 Hz, H_{11}), 8.29 (d, 2H, $J_{12,11}$ = 8.2 Hz, H_{12}), 8.56 (s, 1H, H_9). ^{13}C NMR (50 MHz, $CDCl_3$): δ 13.8 (C_8), 19.2 (C_7), 31.2 (C_6), 67.9 (C_5), 115.0 (C_2), 122.6, 123.9 (C_3, C_{12}), 129.0 (C_{11}), 141.9, 143.2 (C_4, C_{10}), 148.8 (C_{13}), 154.4 (C_9), 158.8 (C_1). HRMS (ESI, IT-TOF) calculated for $C_{17}H_{19}N_2O_3^+$: 299.1390; found: 299.1301.

(*E*)-*N*-(4-butoxyphenyl)-1-(4-fluorophenyl)methanimine (17)

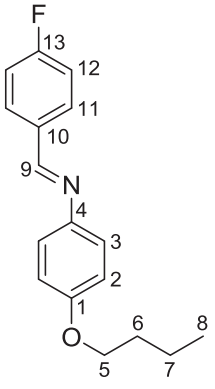

Yield: 74%. Brown solid. Mp: 90.7–91.8 °C. IR (ATR, cm^{-1}) $\bar{\nu}$: 2962, 2938, 2877, 1624, 1600, 1574, 1505, 1472, 1387, 1293, 1216, 1038, 1009. ^1H NMR (200 MHz, $CDCl_3$): δ 0.97 (t, 3H, $J_{8,7}$ = 7.2 Hz, H_8), 1.49 (sex, 2H, $J_{7,6} = J_{7,8}$ = 7.2 Hz, H_7), 1.77 (quin, 2H, $J_{6,5} = J_{6,7}$ = 7.2 Hz, H_6), 3.95 (t, 2H, $J_{5,6}$ = 7.2 Hz, H_5), 6.90 (d, 2H, $J_{2,3}$ = 8.7 Hz, H_2), 7.11 (t, 2H, $J_{12,11} = J_{12,F}$ = 8.5 Hz, H_{12}), 7.19 (d, 2H, $J_{3,2}$ = 8.7 Hz, H_3), 7.85 (dd, 2H, $J_{11,12}$ = 8.5 Hz, $J_{11,F}$ = 5.7 Hz, H_{11}), 8.40 (s, 1H, H_9). ^{13}C NMR (50 MHz, $CDCl_3$): δ 13.8 (C_8), 19.2 (C_7), 31.3 (C_6), 67.8 (C_5), 114.9 (C_2), 115.7 (d, $J_{12,F}$ = 21.8 Hz, C_{12}), 122.1 (C_3), 130.4 (d, $J_{11,F}$ = 8.8 Hz, C_{11}), 133.8 (C_{10}), 144.3 (C_4), 156.5 (C_9), 157.9 (C_1), 164.2 (d, $J_{13,F}$ = 251.1 Hz, C_{13}). HRMS (ESI, IT-TOF) calculated for $C_{17}H_{19}FNO^+$: 272.1445; found: 272.1351.

(*E*)-1-(benzo[*d*][1,3]dioxol-5-yl)-*N*-(4-butoxyphenyl)methanimine (18)

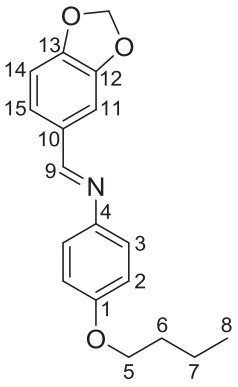

Yield: 69%. Light brown solid. Mp: 96.7–98.0 °C. IR (ATR, cm^{-1}) $\bar{\nu}$: 2956, 2935, 2872, 1623, 1603, 1574, 1502, 1483, 1443, 1382, 1290, 1243, 1209, 1113, 1037, 928, 813, 798. ^1H NMR (200 MHz, $CDCl_3$): δ 0.97 (t, 3H, $J_{8,7}$ = 7.2 Hz, H_8), 1.49 (sex, 2H, $J_{7,6} = J_{7,8}$ = 7.2 Hz, H_7), 1.77 (quin, 2H, $J_{6,5} = J_{6,7}$ = 7.2 Hz, H_6), 3.95 (t, 2H, $J_{5,6}$ = 7.2 Hz, H_5), 5.99 (s, 2H, $OC\underline{H}_2O$), 6.80–6.95 (m, 3H, H_2, H_{14}), 7.11–7.27 (m, 3H, H_3, H_{15}), 7.50 (s, 1H, H_{11}), 8.33 (s, 1H, H_9). ^{13}C NMR (50 MHz, $CDCl_3$): δ 13.8 (C_8), 19.2 (C_7), 31.3 (C_6), 67.8 (C_5), 101.4 ($O\underline{C}H_2O$), 106.6, 108.1 (C_{11}, C_{14}), 114.8 (C_2), 122.0 (C_3), 125.2 (C_{15}), 131.4 (C_{10}), 144.6 (C_4), 148.3, 150.1 (C_{12}, C_{13}), 157.2 (C_9), 157.6 (C_1). HRMS (ESI, IT-TOF) calculated for $C_{18}H_{20}NO_3^+$: 298.1438; found: 298.1341.

(*E*)-*N*-(4-butoxyphenyl)-1-(5-nitrofuran-2-yl)methanimine (19)

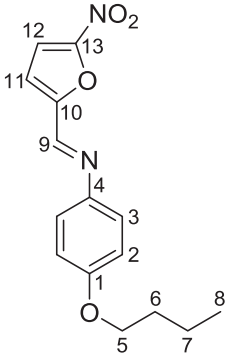

Yield: 85%. Yellow solid. Mp: 137.8–139.3 °C. IR (ATR, cm^{-1}) $\bar{\nu}$: 3144, 2936, 2863, 1619, 1576, 1531, 1498, 1394, 1336, 1293, 1239, 1181, 1115, 1041, 1025, 1011, 838, 815, 739. ^1H NMR (200 MHz, $CDCl_3$): δ 0.98 (t, 3H, $J_{8,7}$ = 7.2 Hz, H_8), 1.50 (sex, 2H, $J_{7,6} = J_{7,8}$ = 7.2 Hz, H_7), 1.78 (quin, 2H, $J_{6,5} = J_{6,7}$ = 7.2 Hz, H_6), 3.99 (t, 2H, $J_{5,6}$ = 7.2 Hz, H_5), 6.93 (d, 2H, $J_{2,3}$ = 7.6 Hz, H_2), 7.14 (s, 1H, H_{11}), 7.30 (d, 2H, $J_{3,2}$ = 7.6 Hz, H_3), 7.41 (s, 1H, H_{12}),

8.40 (s, 1H, H_9). ^{13}C NMR (50 MHz, $CDCl_3$): δ 13.8 (C_8), 19.2 (C_7), 31.2 (C_6), 67.9 (C_5), 113.1, 113.6 (C_{11}, C_{12}), 115.1 (C_2), 122.9 (C_3), 142.4 (C_4), 143.2 (C_9), 152.3, 153.9 (C_{10}, C_{13}), 159.5 (C_1). HRMS (ESI, IT-TOF) calculated for $C_{15}H_{17}N_2O_4^+$: 289.1183; found: 289.1098.

2.2. Antifungal activity

2.2.1. Microorganisms

Candida albicans ATCC 18804, *Candida krusei* ATCC 20298, *Candida tropicalis* ATCC 750, *Candida parapsilosis* ATCC 22019, *Candida glabrata* ATCC 90030 and *Candida dubliniensis* CBS 7987 were procured from the American Type Culture Collection (Manassas, VA). All strains were maintained in the Laboratory of Mycology of the Institute of Biological Sciences at Federal University of Minas Gerais, MG, Brazil, on slopes of Sabouraud dextrose agar (SDA, Difco, Detroit MI, USA) or potato dextrose agar (PDA, Difco) and subcultured every two months.

2.2.2. Susceptibility assay

The antifungal susceptibility test was performed by a broth microdilution assay according to CLSI guidelines M27-A2 (CLSI, 2002). The test compounds were dissolved in dimethylsulfoxide (DMSO) and further diluted with sodium bicarbonate-free RPMI-1640 medium (INLAB, Diadema, SP, Brazil) buffered with 165 mM morpholine propanesulfonic acid (MOPS, Sigma), pH 7.0, supplemented with 4 mM L-glutamine. Each compound was tested in 10 serial concentrations (2048–4.0 μg mL^{-1}). From each dilution, 100 μL was dispensed into flat-bottom 96-well micro titration plates (Cral, Cotia, SP, Brazil). Fluconazole (Sigma-Aldrich, Co, MO, USA) was used as positive control. In addition, growth and sterility control wells were included for each isolate tested. Fungal species were cultured on SDA for 48 h. Concentrations of the fungal inoculums were adjusted spectrophotometrically. Appropriate dilutions were performed using RPMI-1640 medium to obtain a two-fold test inoculum concentration (1 to 5×10^3 cells mL^{-1}). All assays were done in duplicate on at least three different occasions. Inoculum suspensions and solutions of test compounds were mixed (1:1) in sterile flat-bottom 96-well microplates (Difco Laboratories, Detroit, MI, USA). Growth, sterility and toxicity control wells were included for each isolate tested. Microplates were incubated at 35 °C and minimum inhibitory concentration (MIC) endpoints for each microorganism were established at the end of the incubation. MIC values for test compounds corresponded to the lowest concentration necessary to completely inhibit (visually) fungal growth while MIC values for fluconazole were determined as the lowest concentration necessary to inhibit fungal growth by 50%.

3. Results and discussion

3.1. Synthesis of compounds 6–11 and 14–19

Iminecalix[4]arenes **6**–**11** were prepared according to the synthetic approach shown in Scheme 1. Initially, the *p-tert*-butylcalix[4]arene (**1**) was synthesized from the condensation reaction between *p-tert*-butylphenol and formaldehyde, in the presence of sodium hydroxide (Gutsche et al., 1990). Dealkylation of **1** with aluminum chloride and phenol led to compound **2** with 80% yield (Gutsche and Lin, 1986), which was then treated with 1-bromobutane and sodium hydride leading to ether **3** (Nomura et al., 2010). Nitration and subsequent reduction reactions led to intermediate **5** with a yield of 53% (from **3**) (Li et al., 2009; Sansone et al., 2006). Finally, the condensation of **5** with different aromatic aldehydes, assisted by microwave irradiation, resulted in iminecalix[4]arenes **6**–**11** in moderate to good yields. The structural features of the derivatives of the calixarenes were determined from the corresponding IR, ^1H NMR, ^{13}C NMR and mass spectroscopy data.

The main absorption bands in IR spectra of compounds **6**–**11** were recorded in the region of 1600 cm^{-1}, corresponding to the stretching of C═C and C═N bonds, common to all the compounds. The ^1H NMR spectra showed one pair of doublets for methylene bridges at $\delta \sim 3.25$ and ~4.50 ppm, that are characteristics of cone conformation adopted by macrocycles. Singlets of the imino protons (─CH═N─) were observed at δ 7.92–8.28 ppm. For the ^{13}C NMR spectra, the signals for the imino carbons were observed at $\delta \sim 142.2$–161.0 ppm.

The aldimines **14**–**19**, corresponding to respective monomeric units of iminecalix[4] arenes **6**–**11**, were synthesized in a similar manner (Scheme 2). Treatment of 4-nitrophenol with 1-bromobutane and sodium carbonate furnished the compound **12** that was reduced to give the amine **13**. The condensation of **13** with different aromatic aldehydes, assisted by microwave irradiation, provides aldimines **14**–**19** with good yields.

3.2. X-ray crystal structures of iminecalix[4]arenes 7 and 10

Compounds **7** and **10** have been crystallized in the monoclinic space group $P2_1/c$ with one molecule in the asymmetric unit and therefore four ones within their unit cell. Their crystal are very similar, including similar cell constants and volume besides equal lattice symmetry (see crystal data in Experimental section). An illustration of the asymmetric units of compounds **7** and **10** showing the labeling scheme of phenyl rings from the calixarene basis, from one to four (C1 to C6, C8 to C13, C15 to C20, and C22 to C27, in this order), is shown in Figs. 1 and 2. Their crystallographically independent molecule adopts a strongly pinched cone conformation with two upper rim substituents pointing inwards and the other two pointing outwards from the aromatic cavity. This uncommon conformation is driven by an intramolecular π…π interaction between the phenyl rings from the upper rim substituents attached to phenyl rings 1 and 3. These two phenyl rings from either *ortho*-hydroxyphenyl in **7** or benzodioxole in **10** are practically parallel, with a small angle between them of 15.3(5)° in **7** or 0.80(17)° in **10**, besides exhibiting a staggered disposition with a separation between their centroids of 3.912(11) Å in **7** or 3.525(10) Å in **10**. These are relatively short separations supporting the occurrence of the π…π interaction aforementioned. The occurrence of this interaction driving the pinched cone conformation has been already reported in related iminecalix[4]arenes with four propyl groups at the lower rim and 3-pyridyl, 2-thienyl or 2-pyrrolyl as substituents in lieu of substituted phenyl rings in **7** and **10** (Klimentová and Vojtíšek, 2007) as well as in calix[4]arenes with perfluorophenyl ring directly bonded to calixarene platform (Ruban

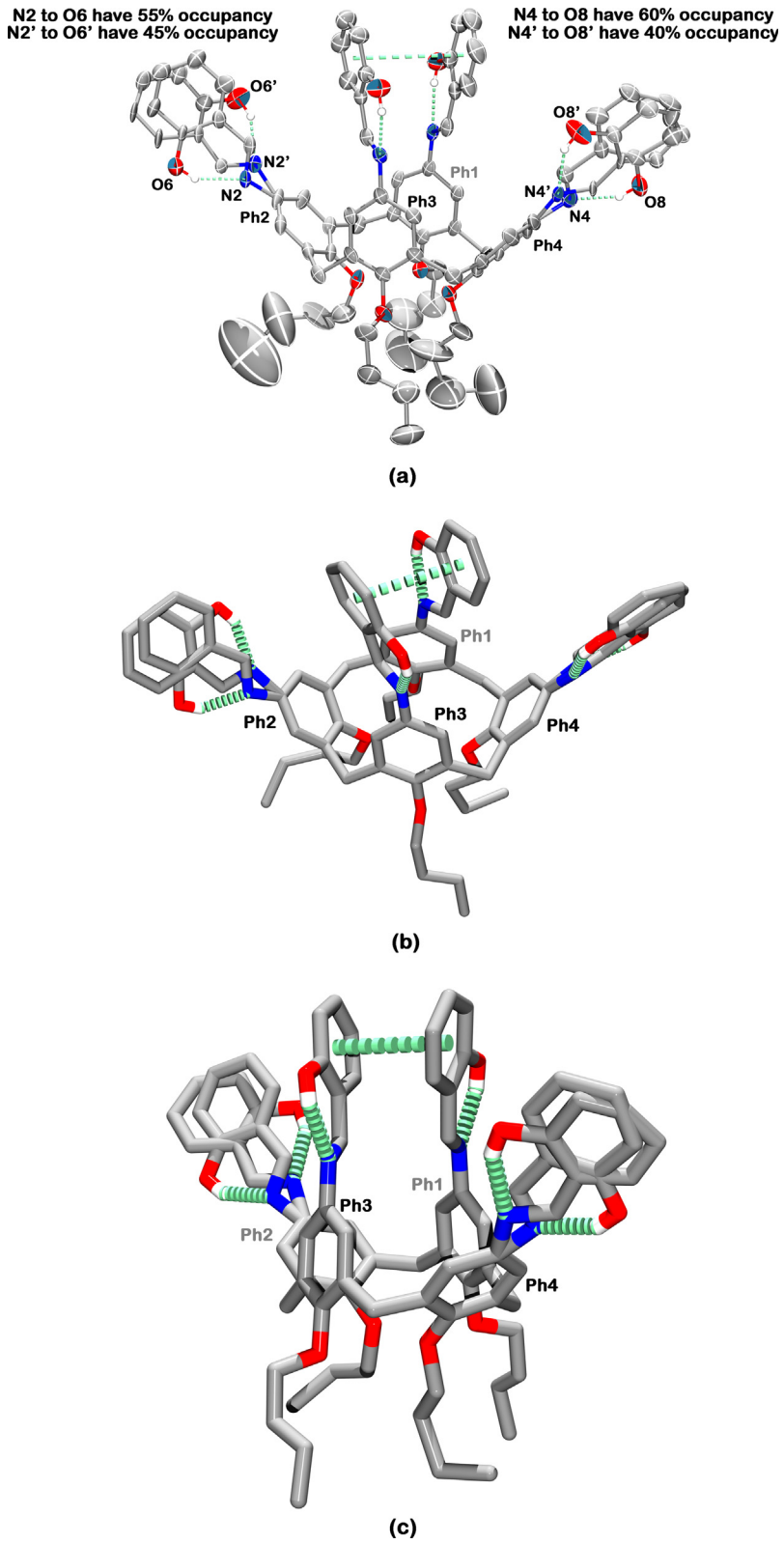

Figure 1 (a) Asymmetric unit of compound **7** drawn with 30% probability ellipsoids. (b) Top and (c) side views of compound **7** in its crystal structure drawn as arbitrary radii sticks. In all panels, hydrogen atoms were omitted for clarity; the labeling scheme of calixarene phenyl rings is shown, and non-covalent intramolecular contacts are shown as dashed green sticks. The two conformations of each upper rim substituent pointing outwards from the cone are also exhibited in all panels [their site occupancy is given in (a)].

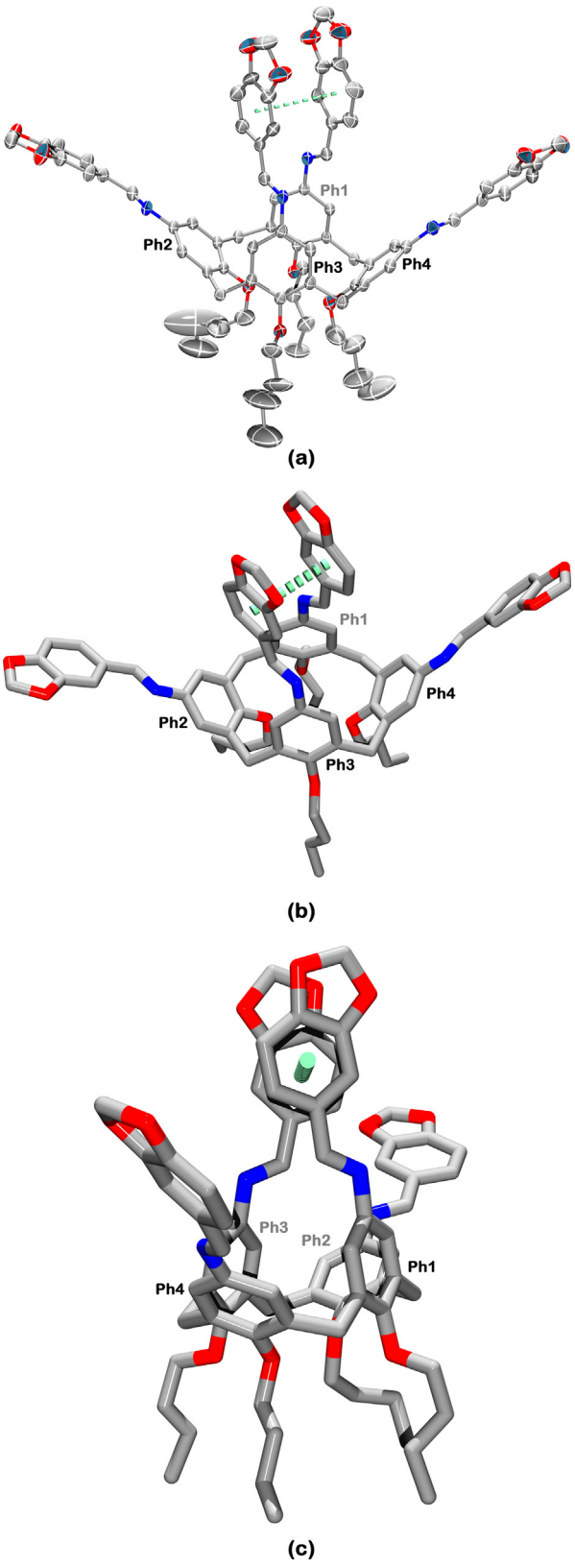

Figure 2 (a) Asymmetric unit of compound **10** drawn with 30% probability ellipsoids. (b) Top and (c) side views of compound **10** in its crystal structure drawn as arbitrary radii sticks. In all panels, hydrogen atoms were omitted for clarity; the labeling scheme of calixarene phenyl rings is shown, and the non-covalent intramolecular contact is shown as dashed green sticks.

et al., 2013). Besides stabilizing the conformation of imine-based calix[4]arenes, π...π interactions are also well-known in their recognition of guests, as occurs in benzimidazole-functionalized calix[4]arenes used as receptors for explosive molecules (Kandpal et al., 2013).

The two π...π stacked phenyl rings are not coplanar in relation to calixarene phenyl rings 1 and 3 to which they are attached, with angles between their least-square planes of 53.2(2)° and 50.8(3)° in **7** or 44.55(13)° and 46.43(11)° in **10**. Such absence of coplanarity between the substituents and calixarene phenyl rings is also found in the two substituents pointing outwards from the aromatic cavity. However, they are a little less bent than those pointing inwards the cone in **10**. The angles between the least-square planes of the calixarene phenyl rings 2 and 4 and their substituents were found to be 48.1(4)° (55% occupancy)/30.2(6)° (45% occupancy) and 50.1(4)° (60% occupancy)/39.6(7)° (40% occupancy) in **7** or 23.36(11)° and 27.23(13)° in **10**.

As can be noted from the last planarity descriptions, both upper rim substituents attached to calixarene phenyl rings 2 and 4 of compound **7** are disordered over two sets of atomic sites with different occupancy factors. This phenomenon is due to the fact that both substituents can adopt two conformations changed by a rotation of approximately 180° on the N—C single bond axis between the substituent and the calixarene fragments (Fig. 1). Additionally, in this compound, all upper rim substituents are stabilized by the formation of $S_1^1(6)$ motifs wherein *ortho*-hydroxyl groups act as intramolecular hydrogen bond donors to the imine nitrogen. The hydrogen bonding geometry of these motifs is shown in Table 1.

Butyl ether moieties bonded to calixarene phenyl rings 1 and 3 are present in similar *syn* conformations in which the carbon chain points outwards from the cone (see Figs. 1c and 2c). On the other hand, corresponding moieties attached to phenyl rings 2 and 4 adopt conformations resembling an *anti*-shaped chain with their bonded oxygen and carbon atoms pointing inwards and the remaining chain directed outwards from the cone.

It is noteworthy that single crystals of the main antifungal compound **11** (see in sequence) were obtained from dimethylformamide solution as large needles (ca. 1 mm in the largest dimension). However, they did not diffract X-rays above 1.5 Å resolution shell, even after using beam source from Cu anode under high exposure time of 60 s. Therefore, we concluded that these crystals did not have long-range order and consequently their crystal structure was not solved in the different X-ray diffraction dataset collected. However, its monoclinic unit cell was determined (a = 14.79(3) Å, b = 33.55(9) Å, c = 13.41(3) Å, β = 100.68(8)°, V = 6581(27) Å^3, see unit cell data for compound **11** in the Experimental section). It was found to be similar to that of the monoclinic unit cell found for the related compounds **7** (a = 12.405(5) Å, b = 30.137(12) Å, c = 17.782(7) Å, β = 101.502(9)°, V = 6514(4) Å^3) and **10** (a = 13.713(4) Å, b = 28.956(9) Å, c = 17.592(6) Å, β = 103.184(18)°, V = 6801(4) Å^3). Therefore, the determined unit cell of **11** is compatible with four molecules thereof, which can be related by symmetry elements of the monoclinic space group $P2_1/c$, as occurs in **7** and **10**. Thus, the unit cell data of **11** are in agreement with its expected molecular structure, in which it adopts a pinched cone conformation observed in its analogs. In order to evaluate and sug-

Table 1 Intramolecular hydrogen bonding geometry of **7**.

Phenyl ring	D—H···A	D—H (Å)	H···A (Å)	D···A (Å)	D—H···A (°)
1	O5—H5···N1	0.82	1.90	2.626(13)	147
2	O6—H6···N2	0.82	1.82	2.56(3)	149
	O6′—H6′···N2′	0.82	1.89	2.62(4)	150
3	O7—H7···N3	0.82	1.90	2.627(13)	147
4	O8—H8···N4	0.82	1.81	2.54(3)	147
	O8′—H8′···N4′	0.82	1.91	2.65(5)	149

gest the presence of the symmetry elements of the $P2_1/c$ space group, we have checked carefully the systematic extinctions. There are only eight $0k0$ reflections. Neither of them has violated the systematic extinction condition for the presence of the 2_1 screw axis symmetry element, *i.e.*, no reflection with odd k was observed (mean $Int./\sigma(Int.) = 0.0$). This analysis suggests the presence of a 2_1 screw axis parallel to the b axis, but this is not conclusive due to the low number of $0k0$ reflections. Likewise, 75 $h0l$ reflections were observed, and neither of them has violated the systematic extinction condition for occurrence of a c-glide perpendicular to the b axis, *i.e.*, no $h0l$ reflection with odd l was detected (mean $Int./\sigma(Int.) = 0.0$). Therefore, the presence of c-glide symmetry element can be stated more surely in this structure. In this way, compound **11** can be arranged in the solid phase with the $P2_1/c$ space group symmetry elements.

3.3. Antifungal activity

As shown in Table 2, wherein the MIC values obtained for each compound are presented, inhibition of all six tested *Candida* strains by iminecalix[4]arenes **6–11** was higher than their respective monomers. This indicates a general increase in antifungal potency of the aldimine monomers upon their cyclization into calixarene platform. Such a conclusion does open a newer perspective of enhancing the antifungal profile of well-known fungicidal compounds through their cyclization or even anchoring them on calixarene grounds. The ratio between the minimal inhibitory concentration (MIC) of a monomer and the corresponding iminecalix[4]arene ranged from 2.05 (MIC ratio between compounds **16** and **8** against *C. parapsilosis*) to 36.50 (MIC ratio between compounds **19** and **11** against *C. albicans*, *C. tropicalis* and *C. parapsilosis*). Compound **11** was the most active among all compounds tested in this study. It exhibited low MIC values comparable to that of positive control (fluconazole), which is a potent inhibitor of fungal growth. The MIC values for compound **11** ranged from 0.05 to 0.11 mmol L^{-1}. Under the same proliferation conditions, MIC values of fluconazole ranged from 0.0008 to 0.10 mmolL^{-1}. Compound **11** (MIC of 0.05 mmolL^{-1}) was even twice more active than fluconazole (MIC of 0.10 mmolL^{-1}) against *C. krusei*.

Inspection of MIC values into either cyclic or monomeric sets of aldimines studied here allowed us to establish some structure-activity relationships. The antifungal potency of the iminecalix[4]arenes with nitro group (**8**) or fluorine (**9**) at 4-position of the substituent phenyl ring has been almost the same against all *Candida* species except against *C. glabrata*. This activity is either 0.21–0.23 mmol L^{-1} or 0.41–0.45 mmol L^{-1}. The decoration of the substituent phenyl ring improves a few of the activities of the iminecalix[4]arenes, since compound **6** presented without any decoration in its substituent phenyl moiety exhibited the highest MIC value (0.48 mmol L^{-1}) among all iminecalix[4]arenes against four *Candida* species. The highest increase in this biological property through the decoration of this phenyl ring occurred in compound **7** present with 2-hydroxyl group (MIC of 0.11 mmol L^{-1} against *C. parapsilosis*). However, decoration of phenyl ring with 3,4-methylenedioxy does not change the antifungal property of the iminecalix[4]arene **10** (MIC of 0.41 mmol L^{-1} against five *Candida* species). Among the monomers, this trend is not observed. Fluoro derivative **17** has presented the same high MIC of 3.77 mmol L^{-1} against all *Candida* species. Undecorated aldimine **14** had the highest MIC of 4.04 mmol L^{-1} against two species, but the compounds **15**, **16** and **18** also showed higher MIC values of 3.80, 3.43 and 3.44 mmol L^{-1}, respectively. The only similarity with iminecalix[4]arenes is the conservation of the lowest MIC values within the set of the monomers for the nitrofuran derivative **19**, which has showed against *C. krusei* a MIC value of 0.22 mmol L^{-1} comparable to that of the calixarene-based compounds. This states that nitrofuran group attached to phenyl moiety increases the antifungal activity of the aldimine and its cyclic analog.

Table 2 Minimal inhibitory concentration (MIC; mmol L^{-1}) of compounds **6–11** and **14–19** against fungal strains.

Fungal strains	Compounds												
	6	**7**	**8**	**9**	**10**	**11**	**14**	**15**	**16**	**17**	**18**	**19**	Flu[a]
C. albicans	0.48	0.45	0.41	0.45	0.41	0.05	2.02	1.90	1.72	3.77	3.44	1.78	0.0008
C. krusei	0.48	0.23	0.21	0.23	0.21	0.05	1.01	1.90	0.86	3.77	1.72	0.22	0.10
C. tropicalis	0.48	0.45	0.41	0.45	0.41	0.05	4.04	3.80	3.43	3.77	3.44	1.78	0.0008
C. parapsilosis	0.24	0.11	0.21	0.23	0.41	0.05	1.01	0.48	0.43	3.77	1.72	1.78	0.007
C. glabrata	0.48	0.23	0.21	0.45	0.41	0.11	4.04	0.95	3.43	3.77	3.44	1.78	0.03
C. dubliniensis	0.24	0.45	0.21	0.23	0.41	0.05	2.02	1.90	1.72	3.77	1.72	0.89	0.0008

[a] Flu stands for fluconazole (positive control).

4. Conclusion

Six iminecalix[4]arenes and their corresponding monomeric units have been synthesized in this study with moderate to good yields. Their structural backbones were confirmed using IR, ^{1}H NMR, ^{13}C NMR and mass spectroscopy data. In addition, crystal structures of two iminecalix[4]arenes provided interesting conformation knowledge thereof. Both compounds have assumed pinched cone conformation kept stable by means of weak intramolecular π. . .π interaction between phenyl rings from upper rim substituents pointing inwards the calixarene cavity. These substituents and those pointing outwards from the cone are twisted relative to calixarene phenyl rings in which they are bonded.

From the antifungal profile, it was possible to conclude that calixarene-based aldimines are more active against *Candida* strains than their monomers. Such an increase in the antifungal property of iminecalix[4]arenes has achieved up to 35.60 times higher activity than the corresponding monomeric molecule. Such a conclusion does open a new perspective of enhancing the antifungal profile of well-known fungicidal compounds through their cyclization or even anchoring them in calixarene grounds. Lastly, the antifungal response of the iminecalix[4]arene with nitrofuran moiety was comparable to that of fluconazole. Our target compound was twice more active than fluconazole against *C. krusei*. This finding highlights the fact that such iminecalix[4]arenes can act as promising antifungal agents. Additionally, it can also guide the search for more powerful antifungal analogs supported on calixarene platform.

Acknowledgments

Authors are thankful to the financial support provided by Fundação de Amparo à Pesquisa do Estado de Minas Gerais (FAPEMIG), Conselho Nacional de Desenvolvimento Científico e Tecnológico (CNPq) and Coordenação de Aperfeiçoamento de Pessoal de Nível Superior (CAPES). ADF, FTM, RBA and MARS are supported by CNPq research fellowship. We also thank FAPEG (Fundação de Amparo à Pesquisa do Estado de Goiás) for the research fellowship (FTM).

References

Abdallah, S.M., Zayed, M.A., Mohamed, G.G., 2010. Synthesis and spectroscopic characterization of new tetradentate Schiff base and its coordination compounds of NOON donor atoms and their antibacterial and antifungal activity. Arab. J. Chem. 3, 103–113.

Amnerkar, N.D., Bhongade, B.A., Bhusari, K.P., 2015. Synthesis and biological evaluation of some 4-(6-substituted-1,3-benzothiazol-2-yl)amino-1,3-thiazole-2-amines and their Schiff bases. Arab. J. Chem. 8, 545–552.

Andriole, V.T., 1999. Current and future antifungal therapy: new targets for antifungal agents. J. Antimicrob. Chemother. 44, 151–162.

Ascioglu, S., Rex, J.H., de Pauw, B., Bennett, J.E., Bille, J., Crokaert, F., Denning, D.W., Donnelly, J.P., Edwards, J.E., Erjavec, Z., Fiere, D., Lortholary, O., Maertens, J., Meis, J.F., Patterson, T.F., Ritter, J., Selleslag, D., Shad, P.M., Stevens, D.A., Walsh, T.J., 2002. Defining opportunistic invasive fungal infections in immunocompromised patients with cancer and hematopoietic stem cell transplants: an international consensus. Clin. Infect. Dis. 34, 7–14.

Bruker, 2012. SAINT. Program for Data Reduction from Area Detectors. BRUKER AXS Inc., 5465 East Cheryl Parkway, Madison, WI 53711-5373, USA.

CLSI, Clinical and Laboratory Standards Institute, 2002. Reference Method for Broth Dilution Antifungal Susceptibility Testing of Yeasts; Approved Standard, second ed. Clinical and Laboratory Standards Institute, Villanova, NCCLS Document M27-A2.

Choi, J.Y., Podust, L.M., Roush, W.R., 2014. Drug strategies targeting CYP51 in neglected tropical diseases. Chem. Rev. 114, 11242–11271.

Consoli, G.M.L., Galante, E., Daquino, C., Granata, G., Cunsolo, F., Geraci, C., 2006. Hydroxycinnamic acid clustered by a calixarene platform: radical scavenging and antioxidant activity. Tetrahedron Lett. 47, 6611–6614.

Consoli, G.M.L., Granata, G., Cafiso, V., Stefani, S., Geraci, C., 2011. Multivalent calixarene-based C-fucosyl derivative: a new Pseudomonas aeruginosa biofilm inhibitor. Tetrahedron Lett. 52, 5831–5834.

da Silva, C.M., da Silva, D.L., Modolo, L.V., Alves, R.B., Martins, C.V.B., de Resende, M.A., de Fátima, A., 2011a. Schiff bases: a short review of their antimicrobial activities. J. Adv. Res. 2, 1–8.

da Silva, C.M., da Silva, D.L., Martins, C.V.B., de Resende, M.A., Dias, E.S., Magalhães, T.F.F., Rodrigues, L.P., Sabino, A.A., Alves, R.B., de Fátima, A., 2011b. Synthesis of aryl aldimines and their activity against Fungi of clinical interest. Chem. Biol. Drug Des. 78, 810–815.

de Fátima, A., Fernandes, S.A., Sabino, A.A., 2009. Calixarenes as new platforms for drug design. Curr. Drug Discov. Tech. 6, 151–170.

de Oliveira, M.C., Reis, F.S., de Fátima, A., Magalhães, T.F.F., da Silva, D.L., Porto, R.R., Watanabe, G.A., Martins, C.V.B., da Silva, D.L., Ruiz, A.L.T.G., Fernandes, S.A., de Carvalho, J.E., de Resende-Stoianoff, M.A., 2012. Synthesis and anti-Paracoccidioides activity of calix[*n*]arenes. Lett. Drug Des. Discov. 9, 30–36.

Deshayes, S., Gref, R., 2014. Synthetic and bioinspired cage nanoparticles for drug delivery. Nanomedicine 9, 1545–1564.

Du, S., Yu, T.-Q., Liao, W., 2015. Structure modeling, synthesis and X-ray diffraction determination of an extra-large calixarene-based coordination cage and its application in drug delivery. Dalton Trans. 44, 14394–14402.

Farrugia, L.J., 2012. WinGX and ORTEP for Windows: an update. J. Appl. Crystallogr. 45, 849–854.

Franco-Paredes, C., Womack, T., Bohlmeyer, T., Sellers, B., Hays, A., Patel, K., Lizarazo, J., Lockhart, S.R., Siddiqui, W., Marr, K.A., 2015. Management of Cryptococcus gattii meningoencephalitis. Lancet Infect. Dis. 15, 348–355.

Gasparto, A.K., Baltazar, L.M., Gouveia, L.F., da Silva, C.M., Byrro, R.M.D., Rachid, M.A., Cunha Júnior, A.S., de Resende-Stoianoff, M.A., de Fátima, A., Santos, D.A., 2015. 2-(Benzylideneamino) phenol: a promising hydroxyaldimine with potent activity against dermatophytoses. Mycopathologia 179, 243–251.

Girmenia, C., Martino, P., de Bernardis, F., Gentile, G., Boccanera, M., Monaco, M., Antonucci, G., Cassone, A., 1996. Rising incidence of *Candida parapsilosis* fungemia in patients with hematologic malignancies: clinical aspects, predisposing factors, and differential pathogenicity of the causative strains. Clin. Infect. Dis. 23, 506–514.

Guo, D.-S., Liu, Y., 2014. Supramolecular chemistry of p-sulfonatocalix[*n*]arenes and its biological applications. Acc. Chem. Res. 47, 1925–1934.

Giuliani, M., Morbioli, I., Sansone, F., Casnati, A., 2015. Moulding calixarenes for biomacromolecule targeting. Chem. Comm. 51, 14140–14159.

Grare, M., Mourer, M., Fontanay, S., Regnouf-de-Vains, J.B., Finance, C., Duval, R.E., 2007. In vitro activity of para-guanidinoethylcalix[4]arene against susceptible and antibiotic-resistant Gram-negative and Gram-positive bacteria. J. Antimicrob. Chemother. 60, 575–581.

Gutsche, C.D., Iqbal, M., Watson, A.T., Heathcock, C.H., 1990. P-tert-Butylcalix[4]arene. Org. Synth. 68, 234–237.

Gutsche, C.D., Lin, L.G., 1986. Calixarenes 12: the synthesis of functionalized calixarenes. Tetrahedron 42, 1633–1640.

Hisaindee, S., Al-Kaabi, L., Ajeb, S., Torky, Y., Iratni, R., Saleh, N., AbuQamar, S.F., 2015. Antipathogenic effects of structurally-

related Schiff base derivatives: structure-activity relationship. Arab. J. Chem. 8, 828–836.
Kamboh, M.A., Bhatti, A.A., Solangi, I.B., Sherazi, S.T.H., Menon, S., 2014. Adsorption of direct black-38 azo dye on p-tert-butylcalix [6]arene immobilized material. Arab. J. Chem. 7, 125–131.
Kandpal, M., Bandela, A.K., Hinge, V.K., Rao, V.R., Rao, C.P., 2013. Fluorescence and piezoresistive cantilever sensing of trinitrotoluene by an upper-rim tetrabenzimidazole conjugate of calix[4] arene and delineation of the features of the complex by molecular dynamics. ACS Appl. Mater. Interf. 5, 13448–13456.
Klimentová, J., Vojtíšek, P., 2007. New receptors for anions in water: synthesis, characterization, X-ray structures of new derivatives of 5,11,17,23-tetraamino-25,26,27,28-tetrapropyloxycalix[4]arene. J. Mol. Struct. 826, 48–63.
Křenek, K., Kuldová, M., Hulíková, K., Stibor, I., Lhoták, P., Dudič, M., Budka, J., Pelantová, H., Bezouška, K., Fišerová, A., Křen, V., 2007. N-Acetyl-D-glucosamine substituted calix[4]arenes as stimulators of NK cell-mediated antitumor immune response. Carbohydr. Res. 342, 1781–1792.
Lappchen, T., Dings, R.P.M., Rossin, R., Simon, J.F., Visser, T.J., Bakker, M., Walhe, P., van Mourik, T., Donato, K., van Beijnum, J.R., van Beijnum, J.R., Griffioen, A.W., Lub, J., Robillard, M.S., Mayo, K.H., Grull, H., 2015. Novel analogs of antitumor agent calixarene 0118: synthesis, cytotoxicity, click labeling with 2-[^{18}F] fluoroethylazide, and in vivo evaluation. Eur. J. Med. Chem. 89, 279–295.
Li, Z.Y., Xing, H.J., Huang, G.L., Sun, X.Q., Jiang, J.L., Wang, L.Y., 2011. Novel supramolecular organocatalysts of hydroxyprolinamide based on calix[4]arene scaffold for the enantioselective Biginelli reaction. Sci. China Chem. 54, 1726–1734.
Li, Z., Ma, J., Chen, J., Pan, Y., Jiang, J., Wang, L., 2009. High-performance liquid chromatography study of the nitration course of tetrabutoxycalix[4]arene at the upper rim: determination of the optimum conditions for the preparation of 5,11,17-trinitro-25,26,27,28-tetrabutoxycalix[4]arene. Chin. J. Chem. 27, 2031–2036.
Macrae, C.F., Bruno, I.J., Chisholm, J.A., Edgington, P.R., McCabe, P., Pidcock, E., Monge, L.R., Taylor, R., van de Streek, J., Wood, P.A., 2008. Mercury CSD 2.0 – new features for the visualization and investigation of crystal structures. J. Appl. Crystallogr. 41, 466–470.
Magalhães, T.F.F., da Silva, C.M., de Fátima, A., da Silva, D.L., Modolo, L.V., Martins, C.V.B., Alves, R.B., Ruiz, A.L.T.G., Longato, G.B., de Carvalho, J.E., de Resende-Stoianoff, M.A., 2013. Hydroxyaldimines as potent in vitro anticryptococcal agents. Lett. Appl. Microbiol. 57, 137–143.
Matar, S.A., Talib, W.H., Mustafa, M.S., Mubarak, M.S., AlDamen, M.A., 2015. Synthesis, characterization, and antimicrobial activity of Schiff bases derived from benzaldehydes and 3,3′-diaminodipropylamine. Arab. J. Chem. 8, 850–857.
Motornaya, A.E., Alimbarova, L.M., Shokova, E.A., Kovalev, V.V., 2006. Synthesis and antiherpetic activity of N-(3-amino-1-adamantyl)calix[4]arenes. Pharm. Chem. J. 40, 68–72.
Mourer, M., Dibama, H.M., Fontanay, S., Grare, M., Duval, R.E., Finance, C., Regnouf-de-Vains, J.B., 2009. P-Guanidinoethyl calixarene and parent phenol derivatives exhibiting antibacterial activities. Synthesis and biological evaluation. Bioorg. Med. Chem. 17, 5496–5509.
Mourer, M., Psychogios, N., Laumond, G., Aubertin, A.M., Regnouf-de-Vains, J.B., 2010. Synthesis and anti-HIV evaluation of water-soluble calixarene-based bithiazolyl podands. Bioorg. Med. Chem. 18, 36–45.
Mourer, M., Dibama, H.M., Constant, P., Daffé, M., 2012. Antimycobacterial activities of some cationic and anionic calix[4]arene derivatives. Bioorg. Med. Chem. 20, 2035–2041.
Nomura, E., Hosoda, A., Takagaki, M., Mori, H., Miyake, Y., Shibakami, M., Taniguchi, H., 2010. Self-organized honeycomb-patterned microporous polystyrene thin films fabricated by calix[4] arene derivatives. Langmuir 26, 10266–10270.
Nucci, M., Marr, K.A., 2005. Emerging fungal diseases. Clin. Infect. Dis. 41, 521–526.
Pfaller, M.A., Pappas, P.G., Wingard, J.R., 2006. Invasive fungal pathogens: current epidemiological trends. Clin. Infect. Dis. 43, S3–S14.
Pfaller, M.A., Diekema, D.J., 2007. Epidemiology of invasive candidiasis: a persistent public health problem. Clin. Microbiol. Rev. 20, 133–163.
Paquet, V., Zumbuehl, A., Carreira, E.M., 2006. Biologically active amphotericin B-calix[4]arene conjugates. Bioconjugate Chem. 17, 1460–1463.
Pappas, P.G., Rex, J.H., Sobel, J.D., Filler, S.G., Dismukes, W.E., Walsh, T.J., Edwards, J.E., 2004. Guidelines for treatment of candidiasis. Clin. Infect. Dis. 38, 161–189.
Patel, M.B., Modi, N.R., Raval, J.P., Menon, S.K., 2012. Calix[4] arene based 1,3,4-oxadiazole and thiadiazole derivatives: design, synthesis, and biological evaluation. Org. Biomol. Chem. 10, 1785–1794.
Pelizzaro-Rocha, K.J., de Jesus, M.B., Ruela-de-Sousa, R.R., Nakamura, C.V., Reis, F.S., de Fátima, A., Ferreira-Halder, C.V., 2013. Calix[6]arene bypasses human pancreatic cancer aggressiveness: downregulation of receptor tyrosine kinases and induction of cell death by reticulum stress and autophagy. Biochim. Biophys. Acta 1833, 2856–2865.
Rizi, K., Murdan, S., Danquah, C.A., Faull, J., Bhakta, S., 2015. Development of a rapid, reliable and quantitative method – "SPOTi" for testing antifungal efficacy. J. Microbiol. Methods 117, 36–40.
Ruban, A.V., Rozhenko, A.B., Pirozhenko, V.V., Shishkina, S.V., Shishkin, O.V., Sikorsky, A.M., Cherenok, S.O., Kalchenko, V.I., 2013. Tetrahedron Lett. 54, 3496–3499.
Sansone, F., Dudic, M., Donofrio, G., Rivetti, C., Baldini, L., Casnati, A., Cellai, S., Ungaro, R., 2006. DNA condensation and cell transfection properties of guanidinium calixarenes: dependence on macrocycle lipophilicity, size, and conformation. J. Am. Chem. Soc. 128, 14528–14536.
Sheldrick, G.M., 2008. A short history of SHELX. Acta Crystallogr. Sect. A 64, 112–122.
Sparber, F., LeibundGut-Landmann, S., 2015. Interleukin 17-mediated host defense against *Candida albicans*. Pathogens 4, 606–619.
Sundriyal, S., Sharma, R.K., Jain, R., 2006. Current advances in antifungal targets and drug development. Curr. Med. Chem. 13, 1321–1325.
Sztanke, K., Maziarka, A., Osinka, A., Sztanke, M., 2013. An insight into synthetic Schiff bases revealing antiproliferative activities in vitro. Bioorg. Med. Chem. 21, 3648–3666.
Tauran, Y., Coleman, A.W., Perret, F., Kim, B., 2015. Cellular and in vivo biological activities of the calix[*n*]arenes. Curr. Org. Chem. 19, 2250–2270.
Ukhatskaya, E.V., Kurkov, S.V., Hjálmarsdóttir, M.A., Karginov, V. A., Matthews, S.E., Rodik, R.V., Kalchenko, V.I., Loftsson, T., 2013. Cationic quaternized aminocalix[4]arenes: cytotoxicity, haemolytic and antibacterial activities. Int. J. Pharm. 458, 25–30.
Varejão, E.V.V., de Fátima, A., Fernandes, S.A., 2013. Calix[*n*]arenes as goldmines for the development of chemical entities of pharmaceutical interest. Curr. Pharm. Des. 19, 6507–6521.
Walsh, T.J., Gonzalez, C., Roilides, E., Mueller, B.U., Ali, N., Lewis, L.L., Whitcomb, T.O., Marshall, D.J., Pizzo, P.A., 1995. Fungemia in children infected with human immunodeficiency virus: new epidemiologic patterns, emerging pathogens, and improved outcome with antifungal therapy. Clin. Infect. Dis. 20, 900–906.
Whibley, N., Gaffen, S.L., 2015. Beyond *Candida albicans*: mechanisms of immunity to non-albicans Candida species. Cytokine 76, 42–52.